Supporting Information for

Effect of Te substitution on crystal structure and transport properties of $AgBiSe_2$ thermoelectric material

Y. Goto[1,*], A. Nishida[1], H. Nishiate[2], M. Murata[2], C. H. Lee[2], A. Miura[3], C. Moriyoshi[4], Y. Kuroiwa[4], and Y. Mizuguchi[1]

1. Department of Physics, Tokyo Metropolitan University, Hachioji 192-0397, Japan
2. National Institute of Advanced Industrial Science and Technology (AIST), Tsukuba, Ibaraki 305-8568, Japan
3. Faculty of Engineering, Hokkaido University, Kita-13, Nishi-8, Kita-ku, Sapporo, Hokkaido 060-8628, Japan
4. Department of Physical Science, Hiroshima University, 1-3-1 Kagamiyama, Higashihiroshima, Hiroshima 739-8526, Japan

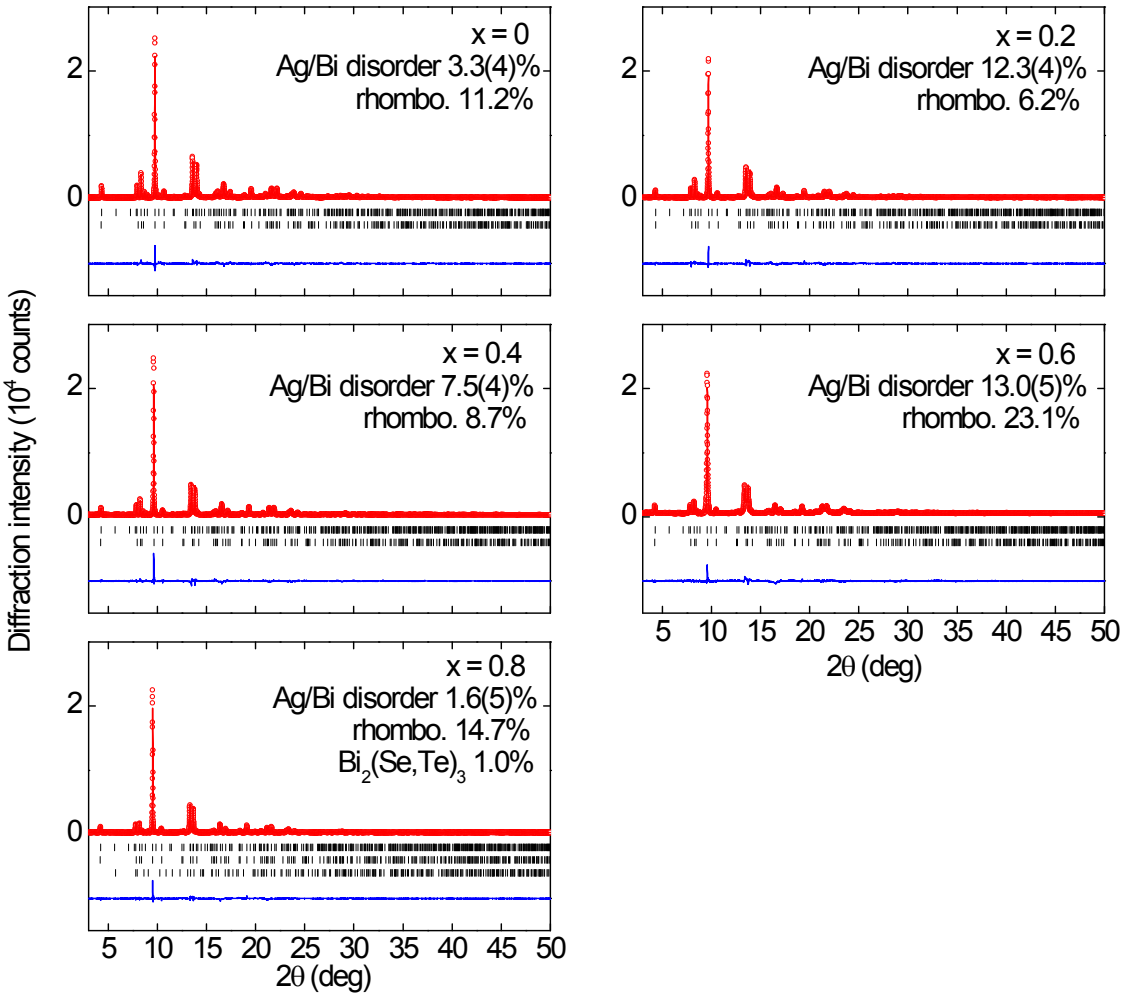

Fig. S1 Synchrotron powder X-ray diffraction (SPXRD) pattern and the results of Rietveld refinement for $AgBiSe_{2-x}Te_x$ (x = 0–0.8) with the wavelength of the radiation beam of 0.496574(1) Å. The circles and solid curve represent the observed and calculated patterns, respectively, and the difference between the two is shown at the bottom. The vertical marks indicate the Bragg diffraction positions for $AgBiSe_{2-x}Te_x$ hexagonal phase (upper) and rhombohedral phase (lower). For x = 0.8, Bragg diffraction positions for $Bi_2(Se,Te)_3$ impurity phase are also shown. Amounts of Ag/Bi anti-site disorder, rhombohedral phase, and $Bi_2(Se,Te)_3$ are denoted in the inset.

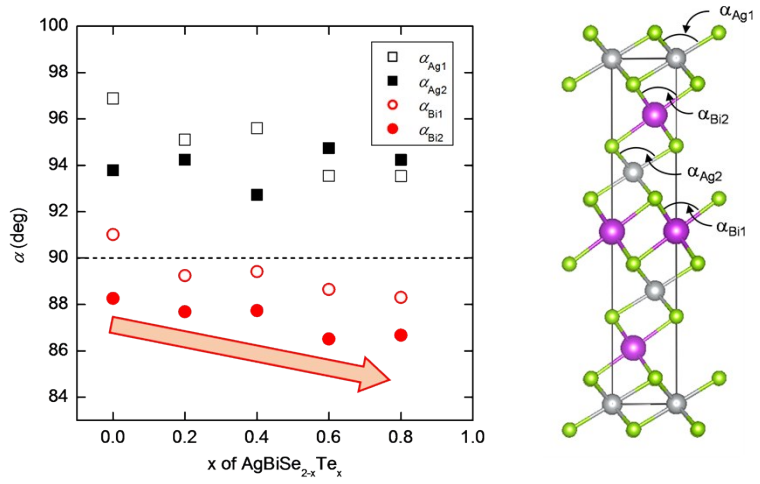

Fig. S2 Bond angles (α) of Ch-M-Ch (Ch = chalcogen, M = Ag or Bi) at room temperature of $AgBiSe_{2-x}Te_x$.

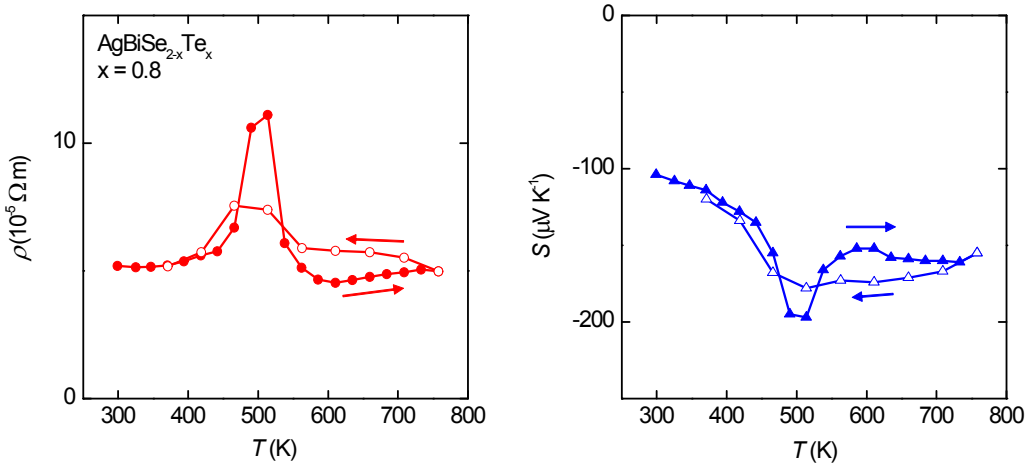

Fig. S3 Temperature dependences of electrical resistivity and Seebeck coefficient of $AgBiSe_{2-x}Te_x$ (x = 0.8). Close and open symbols denote the measurement results for heating and cooling cycle.

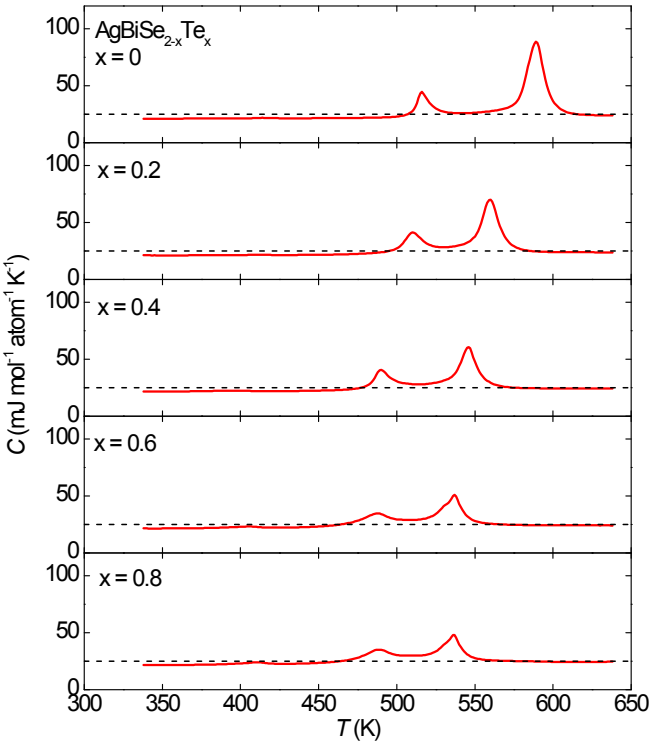

Fig. S4 Temperature dependence of specific heat measured using DSC for $AgBiSe_{2-x}Te_x$. Dashed lines represent the value calculated using Dulong-Puti law.